Adsorption of Chromate and Arsenate by Amino-Functionalized MCM-41 and SBA-1

Hideaki Yoshitake,*,† Toshiyuki Yokoi,†,‡ and Takashi Tatsumi‡

Graduate School of Environment and Information Sciences, Yokohama National University, 79-7 Tokiwadai, Hodogaya-ku, Yokohama 240-8501, Japan, and Division of Material Sciences, Graduate School of Engineering, Yokohama National University, 79-5 Tokiwadai, Hodogaya-ku, Yokohama 240-8501, Japan

Received March 19, 2002. Revised Manuscript Received August 29, 2002

We report the characteristics of aminosilane-grafted mesoporous silicas as adsorbents of oxyanions in acidic conditions. Mono-, di-, and triamino-functionalized silicas were prepared to examine the influence of amino group density. The triaminosilane-grafted mesoporous silica adsorbed more chromate and arsenate than expected from the increased number of sites, suggesting stable complex formations. Functionalized SBA-1 showed larger adsorption capacities than MCM-41 derivatives. The adsorption capacity was independent of the average surface density of monoamino groups, demonstrating domain formation of fixed silanes. These structural characteristics on molecular and meso scales may offer insights into understanding the mechanism of heterogeneous oxyanion capture by amino-functionalized solids, which are promising inexpensive reagents for reducing toxic anion pollution.

Introduction

The risk of exposure to toxic oxyanions in groundwater is a rising environmental problem worldwide. Among these anions, arsenate and chromate are particularly hazardous. The EPA maximum contaminant level for As in drinking water is 10 μg·dm^{-3}, and naturally occurring excessive arsenic has been widely detected in wells in the Chikugo plain, Japan.[1] Moreover, chronic toxicity has been reported as causing the emergence of blackfoot disease on the south-western coast of Taiwan,[2,3] and, more recently, of various cancers in Bangladesh.[4] Chromium is used in industries such as electroplating and tanning, and untreated effluents from such industries pollute the groundwater.[5,6] A simple and low-cost device is necessary for the remediation of water in areas dependent on wells.

Adsorption of toxic species on solid surfaces is considered to be an effective method for improving the environment. The adsorption uptake and kinetics of aqueous arsenic anions have been investigated for metal-impregnated activated carbon,[7−9] coral limestone,[10] lanthanum compounds,[11] ferric (hydr)oxides,[12−15] iron,[16] active alumina,[17] clays,[18] and various biological products.[19−23] Titanium oxide on clay,[24] γ-alumina,[25] bentonite,[26] and biomass [27−29] have also attracted interest. These studies have been aimed at searching for effective adsorbents or the development of geochemical models of arsenic distribution. Conventional porous solids, such as coconut coir,[30] zeolite,[31−33] and clay

* Corresponding author.
† Graduate School of Environment and Information Sciences.
‡ Graduate School of Engineering.

(1) Kondo, H. *Mizukankyo Gakkaishi*, **1997**, *20*, 6.
(2) Sen, Y. S.; Shen, C. S. *J. Water Pollut. Control Fed.* **1964**, *36*, 281.
(3) Chen, S. L.; Dzeng, S. R.; Yang, M. H.; Chiu, K. H.; Shieh, G. M.; Wai, C. M. *Environ. Sci. Technol.* **1994**, *28*, 877−881.
(4) Nickson, R.; McArthur, J.; Burgess, W.; Ahmed, K. M.; Ravenscroft, P.; Rahman, M. *Nature* **1998**, *395*, 338.
(5) Lawrence, M. M. *Environ. Sci. Technol.* **1981**, *15*, 1482−1984.
(6) Tavani, E. L.; Volzone, C. *J. Soc. Leather Technol. Chem.* **1997**, *81*, 143−148.
(7) Huang, C. P.; Fu, P. L. *J. Water Pollut. Control Fed.* **1984**, *56*, 233.
(8) Huang, C. P.; Vane, L. M. *J. Water Pollut. Control Fed.* **1989**, *61*, 1596.
(9) Rajakovic, L. V.; Mitovic, M. M. *Environ. Pollut.* **1992**, *75*, 279.
(10) Ohki, A.; Nakayachigo, K.; Naka, K.; Maeda, S. *Appl. Organomet. Chem.*, **1996**, *10*, 747.
(11) Tokunaga, S.; Wasay, S. A.; Park, S.-W. *Water Sci. Technol.* **1997**, *35*, 71.
(12) Gao, Y.; Mucci, A. *Geochim. Cosmochim. Acta* **2001**, *65*, 14.
(13) Lumsdon, D. G.; Meeussen, J. C. L.; Paterson, E.; Garden, L. M.; Anderson, P. *Appl. Geochem.* **2001**, *16*, 571.
(14) Nilsson, N.; Persson, P.; Lovgren, L.; Sjoberg. S. *Geochim. Cosmochim. Acta* **1996**, *60*, 4385.
(15) Geelhoed, J. S.; Hiemstra T.; van Riemsdijk, W. H. *Geochim. Cosmochim. Acta* **1997**, *61*, 2389.
(16) Su, C.; Puls, R. W. *Environ. Sci. Technol.* **2001**, *35*, 1487.
(17) Lin, T. F.; Wu, J. K. *Water Res.* **2001**, *35*, 2049.
(18) Elizalde-Gonzales, M. P.; Mattusch, J.; Wennrich, R.; Morgenstern, P. *Microporous Mesoporous Mater.* **2001**, *46*, 277.
(19) Cullen, W. R.; Reimer, K. J.; *Chem. Rev.* **1989**, *89*, 713 and references therein.
(20) Chen, J.; Yiacoumi, S. *Sep. Sci. Technol.* **1997**, *32*, 51.
(21) Elson, C. M.; Davies, D. H.; Hayes, E. R. *Water Res.* **1980**, *14*, 1307.
(22) Muzzarelli, R. A. A.; Tanfani, F.; Emanuelli, M. *Carbohydr. Polym.* **1984**, *4*, 137.
(23) Dambies, L.; Guibal, E.; Roze, A. *Colloids Surf. A* **2000**, *170*, 19.
(24) Weng, C. H.; Wang, J. H.; Huang, C. P. *Water Sci. Technol.* **1997**, *35*, 55.
(25) Wu, C. H.; Lo, S. L.; Lin, C. F. *Colloids Surf. A* **2000**, *166*, 251.
(26) Khan, S. A.; Rehman, R. Khan, M. A. *Waste Manag.* **1995**, *15*, 271.
(27) Low, K. S.; Lee, C. K.; Lee, C. Y. *Appl. Biochem. Biotechnol.* **2001**, *90*, 75.
(28) Nakano, Y.; Takeshita, K.; Tsutsumi, T. *Water Res.* **2001**, *35*, 496.
(29) Dean, S. A.; Tobin, J. M. *Resour. Conserv. Recycl.* **1999**, *27*, 151.
(30) Baes, A. U.; Okuda, T.; Nishijima, W.; Shoto, E.; Okada, M. *Water Sci. Technol.* **1997**, *35*, 89.
(31) Haggerty, G. M.; Bowman, R. S. *Environ. Sci. Technol.* **1994**, *28*, 452−458.

10.1021/cm0202355 CCC: $22.00
Published on Web 10/09/2002

minerals,[34] modified with amines have been applied to the removal of chromate and arsenate. These composite materials, with ill-defined structures, showed low absorption capacities. The required properties of the ideal adsorbent are uniformly accessible pores, high density of adsorption sites, and environmental adaptability. However, natural minerals and biomass do not satisfy these geometric conditions.

A decade has passed since the discovery of a family of novel mesoporous molecular sieves synthesized with the aid of micelle templates.[35−38] A huge number of works have been devoted to the materials in this new category. The pore structure is unique, as they form well-ordered periodic structures, and, in addition, the pore size is controllable by varying the template molecule or using additives such as trimethylbenzene.[39,40] Studies of the chemistry of molecules in the confined mesospace has flourished thereafter.[41, 42]

The characteristics of mesoporous molecular sieves are attractive to researchers seeking adsorbents of low concentration ions in the environment. Because the efficient adsorption of a certain target ion is not expected on silica surfaces, the strategy of functionalization of the surface must be designed for oxyanion adsorption. The high density of silanol groups (from 0.5 to 3.0 OH per nm^2) [43] helps to fix large amounts of silanes with an adsorption activity on to a silica surface. The adsorption of toxic metal cations has been explored for functional groups fixed on mesoporous silicas. The divalent cations (Cu, Zn, Cr, and Ni) present in wastewater are adsorbed to a greater extent on amino-functionalized SBA-15 than on thiol-functionalized SBA-15, whereas Hg^{2+} is preferably adsorbed on thiol-functionalized SBA-15.[44] The mercury adsorption on the thiol-functionalized mesoporous silicas has been intensively studied, probably because of the general environmental impact.[45−48] One of these studies showed that formation of almost a monolayer of $Si-CH_2-CH_2-CH_2-SH$ was followed by bridging by $Hg-O-Hg$ units at sulfur atoms.[45]

An advantage of this type of strategy is that the adsorption site has a molecular nature so that the adsorption capacity can be estimated on the basis of a certain stoichiometry. However, it was demonstrated that the ratio of Hg to S depended on the kind of mesoporous silica.[46] This was explained by the lack of uniformity of the structure that may occur but has scarcely been investigated in the synthesis of coordination structures in the mesopores. The problem of the stoichiometry is clearly important in the design of the adsorbent because the uptake of the pollutant ions is, approximately, the product of surface area, surface density of adsorption sites, and the stoichiometry. Numerous works were published on the syntheses of metal-coordinated functionalized mesoporous silicas[42,49−54] which suggest the structure of the adsorption site capturing cations (or anions).

Unlike cation capture by amino- or thiol- groups, the studies of anion adsorptions by functional groups fixed in the pores of mesoporous silicas are rare. Recently, Fryxell et al. showed that diamino-functionalized MCM-41 exhibited a marked capacity for adsorption of Cu^{2+}.[55] The leaching of Cu^{2+} during the adsorption is not apparently significant because of the high affinity of the en. ligand. However, the potential risk due to the toxicity of Cu would appear in the disposal and regeneration of used adsorbent. Surface amino groups are positively charged in acidic conditions where most contamination of the environment by oxyanions occur. We considered that bare amino groups on the solid surfaces could interact with anions in the acidic conditions without the help of other metal cations. In this study, the adsorptions of arsenate and chromate on protonated amino groups fixed on mesoporous silicas were investigated with respect to the removal efficiency from the solution and the adsorption capacity in terms of the stoichiometry of anion/N. The number of the amines (i.e., mono-, di-, and triamino forms) in an organic chain, the surface density of functionalized groups, and the mesoporous framework structure were changed in order to clarify the effect of the density of amino groups on molecular and nano scales as well as the nature of the porous structures. We intended to explore the mode of interaction of the adsorption sites and oxyanions in the mesopores with well-defined structures, and find a key to the design of effective adsorbents of oxyanions.

Experimental Section

Chemicals. Mesoporous silicas were synthesized with tetraethyl orthosilicate (TEOS, Tokyo Kasei Kogyo Co., Ltd., reagent grade) as a silica source. Dodecyltrimethylammonium chloride (DTMACl, >98%) was purchased from Tokyo Kasei Co. Ltd. Cetyltriethylammonium bromide (CTEABr) was synthesized by the reaction of cetyl bromide ($C_{16}H_{33}Br$, Tokyo

(32) Li, Z.; Bowman, R. S. *Environ. Sci. Technol.* **1997**, *31*, 2407−2412.
(33) Li, Z. *J. Environ. Qual.* **1998**, *27*, 240−242.
(34) Krishna, B. S.; Murty, D. S. R.; Prakash, J. B. S. *Appl. Clay Sci.* **2001**, *20*, 65.
(35) Yanagisawa, T.; Shimizu, T.; Kuroda, K.; Kato, C. *Bull. Chem. Soc. Jpn.* **1990**, *63*, 988.
(36) Inagaki, S.; Fukushima, Y.; Kuroda, K. *J. Chem. Soc., Chem. Commun.* **1993**, 680.
(37) Kresge, C. T.; Leonovicz, M. E.; Roth, W. J.; Vartuli, J. C.; Beck, J. S. *Nature* **1992**, *710*, 359.
(38) Beck, J. S.; Vartuli, J. C.; Roth, W. J.; Leonowicz, M. E.; Kresge, C. T.; Schmitt, K. D.; Chu, C. T.-W.; Olson, D. H.; Sheppard, E. W.; McCullen, S. B.; Higgins J. B.; Schlenker, J. L. *J. Am. Chem. Soc.*, **1992**, *114*, 10834.
(39) Ying, J. Y.; Mehnert, C. P.; Wong, M. S. *Angew. Chem., Int. Ed.* **1999**, *38*, 56.
(40) Corma, A. *Chem. Rev.* **1997**, *97*, 2373.
(41) Thomas, J. M. *Angew. Chem., Int. Ed.* **1999**, *38*, 3588.
(42) Moller, K.; Bein, T. *Chem. Mater.* **1998**, *10*, 2950.
(43) Zhao, X. S.; Lu, G. Q.; Whittaker, A. J.; Millar, G. J.; Zhu, H. Y. *J. Phys. Chem. B* **1997**, *101*, 6525 and references therein.
(44) Liu, A. M.; Hidajat, K.; Kawi, S.; Zhao, D. Y. *Chem. Commun.* **2000**, 1145.
(45) Feng, X.; Fryxell, G. E.; Wang, L. Q.; Kim, A. Y.; Liu, J.; Kemner, K. M. *Science* **1997**, *276*, 923.
(46) Mercier, L.; Pinnavaia, T. J. *Environ. Sci. Technol.* **1998**, *32*, 2749.
(47) Brown, J.; Richer, R.; Mercier, L. *Microporous Mesoporous Mater.* **2000**, *37*, 41.
(48) Nooney, R. I.; Kalyanaraman M.; Kennedy, G.; Maginn, E. J. *Langmuir* **2001**, *17*, 528.
(49) Holland, B. T.; Walkup, C.; Stein, A. *J. Phys. Chem. B* **1998**, *102*, 4301.
(50) Sutra, P.; Brunel, D. *Chem. Commun.* **1996**, 2485.
(51) Lau, S. H.; Caps, V.; Yeung, K. W.; Wong, K. Y.; Tsang, S. C. *Microporous Mesoporous Mater.* **1999**, *32*, 279.
(52) Evans, J.; Zaki, A. B.; El-Sheikh, M. Y.; El-Safty, S. A. *J. Phys. Chem. B* **2000**, *104*, 10271.
(53) Diaz, J. F.; Balkus, K. J., Jr. *Chem. Mater.* **1997**, *9*, 61.
(54) Park, D. H.; Park, S. S.; Choe, S. J. *Bull. Korean Chem. Soc.* **1999**, *20*, 291.
(55) Fryxell, G. E.; Liu, J.; Hauser, T. A.; Nie, Z.; Ferris, K. F.; Mattigod, S.; Gong, M.; Hallen, R. T. *Chem. Mater.* **1999**, *11*, 2148.

Kasei Kogyo Co., Ltd., >96%) with triethylamine ($(C_2H_5)_3N$, Tokyo Kasei Kogyo Co., Ltd., >99%) with refluxing for 7 d in acetone. The product was recrystallized from an acetone solution and dried at 333 K in vacuo. Reagent grade trimethylammonium hydroxide (TMAOH, Aldrich) was used as received. 3-Aminopropyltrimethoxysilane ($H_2NCH_2CH_2CH_2Si(OCH_3)_3$) and [1-(2-amino- ethyl)-3-aminopropyl]trimethoxysilane ($H_2NCH_2CH_2NHCH_2CH_2CH_2Si(OCH_3)_3$) were purchased from Tokyo Kasei Kogyo Co., Ltd. Their purities were >98 and >95%, respectively. (Trimethoxysilyl)propyldiethylenetriamine ($H_2NCH_2CH_2HNCH_2CH_2NHCH_2CH_2CH_2(OCH_3)_3$) was obtained from Aldrich. Potassium arsenate (KH_2AsO_4, Pr.G.) and potassium chromate (K_2CrO_4, >99%) were the products of Wako Pure Chemical Industries Ltd. *Arsenate and chromate solutions are toxic and should be treated wearing impermeable gloves and goggles in order to avoid contact with skin and eyes.*

Synthesis of MCM-41. TEOS, DTMACl and TMAOH were mixed in water and the solution was stirred for 4 h at room temperature. The composition of the gel mixture was Si: DTMACl: TMAOH: H_2O = 1:0.6:0.3:60. The white precipitate was filtered and dried at 393 K. This as-synthesized powder was calcined at 903 K for 4 h.

Synthesis of SBA-1. Tetraethyl orthosilicate was added to an aqueous solution of CTEABr acidified with HCl and was stirred vigorously at 273 K for 4 d. The white precipitate was filtered and dried at 393 K. This as-synthesized powder was calcined at 903 K for 4 h. The composition of the gel mixtures was 0.13 CTEABr:1 TEOS:2.5 HCl:125 H_2O.

Functionalization of Mesoporous Silicas. These mesoporous silicas were dehydrated at 423 K in a vacuum to remove water molecules adsorbed on the surface, and were then stirred vigorously in toluene containing 3-aminopropyltrimethoxysilane, [1-(2-aminoethyl)-3-aminopropyl]trimethoxysilane, or (trimethoxysilyl)propyldiethylenetriamine. These solutions were heated to 383 K in dry nitrogen for 6 h. The powder was collected by filtration, washed with 2-propanol for 2 h, and dried at 373 K. Then, 100 mg of the powder was stirred in 100 mL of 0.1 M HCl for 6 h without heating. This process converts amino groups into ammonium salts. These mono-, di-, and triamino functionized silica chlorides are denoted by N-, NN-, and NNN- mesoporous silicas, respectively, where mesoporous silica is MCM-41 or SBA-1.

Characterization. The periodic structure of the framework was confirmed by powder X-ray diffraction (XRD, with an XL Labo diffractometer, MAC Science Co., Ltd.) with Cu K_α radiation at 40 kV and 20 mA. Nitrogen adsorption−desorption isotherms were recorded using a BELSORP 28SA (BEL Japan Inc.) after the sample was evacuated at 473 K for 2 h. IR spectra of modified and unmodified mesoporous silicas were measured with a Perkin-Elmer system 2000 spectrometer in transmission mode. The powder was molded into self-supporting disks, which were directly mounted in the sample holder of the spectrometer. Proton-decoupled ^{29}Si MAS NMR spectra were recorded on a JEOL JNM-LA400WB 400 MHz spectrometer at 79.4 MHz and a sample spinning frequency of 5 kHz.

Anion Adsorption. The standard procedure in adsorption experiments was as follows. A 50-mg portion of modified mesoporous silicas was stirred for 10 h in 100 mL of aqueous solution of K_2CrO_4 or KH_2AsO_4. The adsorption was completed within 5 min for most concentrations we investigated. However, when the concentration of oxyanion was 1700 ppm, which is three times higher than the capacity of the adsorbent, it needed 5 h at maximum. Thus, the specific adsorptions were measured at 5 h. The solution was filtered to remove solids and analyzed by induced coupled plasma (ICP) spectrometry. The typical pHs of the solutions at the beginning were 8−9 and 6−7, and, after adsorptions, they changed to 7−8 and 3−4 for chromate and arsenate, respectively. In this pH range, the dominant arsenate and chromate species in the aqueous solution are CrO_4^{2-} and $H_2AsO_4^-/HAsO_4^{2-}$, respectively.

Results and Discussion

Structure of Functionalized Mesoporous Silicas. Figure 1 compares the X-ray diffraction patterns of the mesoporous silicas before and after functionalization with [1-(2-aminoethyl)-3-aminopropyl] trimethoxysilane. In the pattern of MCM-41, a dominant (100) peak with small (110) and (200) reflections, are attributed to the 2D-hexagonal structure (*p6mm*).[38] Diaminosilane grafting to MCM-41 caused a considerable decrease in the XRD intensity. The reflections due to higher indices almost disappeared. These changes in the figure are due to a partial loss of the space correlation of the pores. This kind of resultant disorder in silica mesostructures has been commonly observed in studies of the silylation of mesoporous silicas.[46,52,56,57] After protonation, the peak again decreased, implying that the mesostructure of MCM-41 is sensitive to both the silylation reaction and acid treatment. The characteristic reflections indexed to (200), (210), and (211) and unresolved peaks of higher ones were clearly observed in SBA-1 (*Pm*3*n*).[58] Grafting and acid treatment gradually decreased the peak intensities of this pattern. Although the unresolved peaks of higher indices almost disappeared after the silylation, more than half of the intensities of untreated SBA-1 are retained in (200), (210), and (211) reflections. This implies that the mesostructural ordering of SBA-1 is less sensitive to silylation and acid treatment than that of MCM-41. The decrease in the meso-orders was probably caused by siloxane bond dissociations by methanol at high temperature, or from the acid.

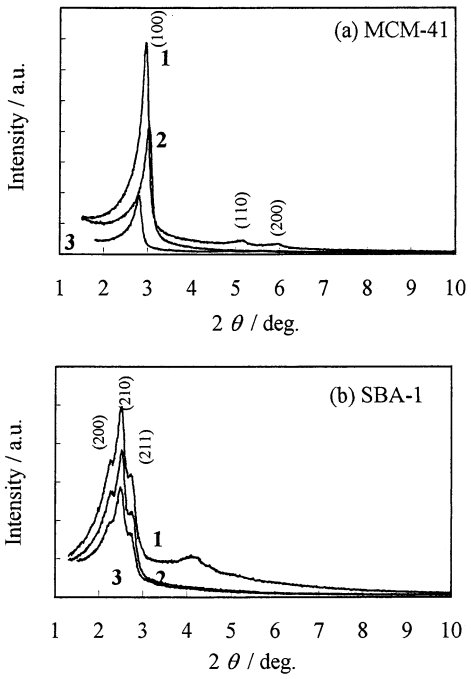

Figure 1. X-ray diffraction patterns of mesoporous silicas prior to (1) and following (2) functionalization with [1-(2-aminoethyl)-3-aminopropyl]trimethoxy silane, and after treatment in hydrochloric acid (3).

The nitrogen adsorption isotherms of the treated and untreated mesoporous silicas are shown in Figure 2. The features of the curves for MCM-41 and SBA-1 contain linear to step-shaped uptakes at partial pressures between 0.1 and 0.8. These features are indicative of

(56) Zhao, X. S.; Lu, G. Q. *J. Phys. Chem. B* **1998**, *102*, 1556.
(57) Autochshuk, V.; Jaroniec, M. *Chem. Mater.* **2000**, *12*, 2496.
(58) Che, S.; Sakamoto, Y.; Terasaki, O.; Tatsumi, T. *Chem. Mater.* **2001**, *13*, 2231.

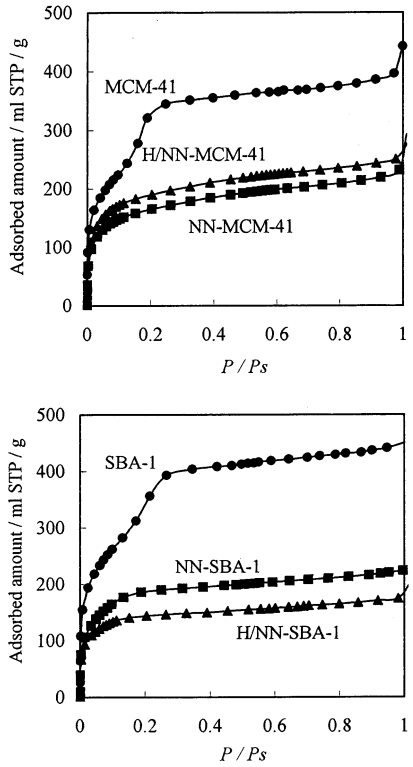

Figure 2. Nitrogen adsorption isotherms of mesoporous silicas prior to (MCM-41 and SBA-1) and following (NN-MCM-41 and NN-SBA-1) functionalization with [1-(2-aminoethyl)-3-aminopropyl]trimethoxy silane, and after treatment in hydrochloric acid (H/NN-MCM-41 and H/NN-SBA-1).

the presence of mesopores. Upon grafting [1-(2-aminoethyl)-3-aminopropyl]trimethoxysilane to the framework walls and successive H^+ treatment, significant decreases in the surface area, pore volume, and pore size were observed. This resulted from liganding diamino groups in the framework channels. The BET surface area (S_{BET}), total pore volume (V_p) and most probable pore size ($2R_P$) in BJH distributions are listed in Table 1 with the results of elemental analysis, the C to N ratio; the N content is given as mmol per g of powder and surface density. These parameters for mono and triamino silanes were also determined as for diaminosilane.

The BET surface area, total pore volume, and the most probable pore diameter decreased with increasing number of nitrogen atoms in the silane for both MCM-41 and SBA-1. These changes in mesopore structure are explained qualitatively by the exclusion volume of the surface organic groups as is widely observed in grafting.[43,46,47,59] However, we observed a few points in Table 1 which cannot be clarified well by this simple explanation. The change in surface area and pore volume was small when monoaminosilane was fixed on MCM-41 while diamino and triamino functionalizations resulted in significant reductions of these parameters. In the case in SBA-1, the decreases in S_{BET} and V_P after grafting (trimethoxysilyl)propyldiethylenetriamine were considerable, from 1221 to 126 $m^2 \cdot g^{-1}$ and 281 to 36 $mm^3 \cdot g^{-1}$, respectively. The blockage of pores to penetrating nitrogen is likely to be more important than the destruction of mesostructures in SBA-1 whose pores do not have a straight channel structure as in MCM-41 but a cage-type one. The mechanism of the blockage at the pore windows is supported by the observation that the attached silane per unit weight decreases with the increasing size of the molecule (1.46, 1.38, and 1.18 $mmol \cdot g^{-1}$ for N-, NN-, and NNN-MCM-41, respectively, and 1.90, 1.67, and 1.46 $mmol \cdot g^{-1}$ for N-, NN-, and NNN-SBA-1, respectively).

The previous work on diamino-silylation of MCM-41[55] showed a significantly larger coverage of silane (3.3 $mmol \cdot g^{-1}$ or 4.9 silane per/nm^2) than the results in Table 1 (1.38 $mmol \cdot g^{-1}$ or 0.65 silane per/nm^2). This difference probably arises from the difference in pore sizes, 6 vs 2.63 nm, respectively, and the water treatment just before the silylation. The larger pore can avoid a steric congestion of the silane molecules as mentioned above. The pretreatment with water easily induces the full coverage of adsorbed water, which allows the formation of hydroxy silanes to result in the assembly and aggregation of the molecules that are still mobile on the surface and finally fixed by the silanol or siloxane. Thus, in the presence of water, the silane molecules are attached beyond the density of isolated silanols. In this work, the mesoporous silicas were dried before the silylation, and the density of silane was not as high as that of surface silanols.

Figure 3 shows the infrared spectra of MCM-41 and SBA-1 prior to and following grafting by [1-(2-aminoethyl)-3-aminopropyl]trimethoxysilane. Several silanol bands at 3667, 3647, and 3436 cm^{-1} are not well resolved in the spectrum of MCM-41, while a sharp absorption is observed at 3742 cm^{-1}. The sharp band has been assigned to isolated Si−OH and the others resulted from the contributions of hydrogen bonded silanols.[29,43,60] Bands at 2928, 2858, 1669, 1604, 1458, and 1352 cm^{-1} appear at the expense of the band at 3742 cm^{-1} after silylation, which are assigned to C−H asymmetric stretching, C−H symmetric stretching, NH_2 scissor, NH_2 scissor, CH_2 scissor, and CH_3 bending vibrations, respectively. The band positions are similar to those reported in the literature.[53,54] The presence of the CH_3 bending mode suggests a small amount of remaining $-OCH_3$. A quite broad band is observed in the region of OH absorption in SBA-1. The peak maximum is found around 3724 cm^{-1} which can be assigned to isolated silanol. This band decreased after silylation leaving a broad band around 3648 cm^{-1}. Bands at 1662, 1609, 1450, 1370, and 1349 cm^{-1} were observed in the spectrum after grafting, which are attributed to NH_2 scissor, NH_2 scissor, CH_2 scissor, CH_3 bending, and CH_3 bending vibrations, respectively. The similar positions of the bands appearing at 1300−1700 cm^{-1} region and a splitting feature of the band for NH_2 scissors suggest that the similar structure of the functional group was likely to be formed on MCM-41 and SBA-1.

Figure 4 shows the ^{29}Si NMR spectra of NN-MCM-41 and NN-SBA-1. The peaks appeared at −58, −67, −100 (*sh*), and −111 ppm which are assigned to Si(OH)R$(OSi)_2$ (T^2), SiR$(OSi)_3$ (T^3), Si(OH)$(OSi)_3$ (Q^3), and $Si(OSi)_4$ (Q^4).[45] An isolated species, Si(OH)R(OCH_3)(OSi), which is expected to appear around −50 ppm, was

(59) Van Rhijn, W. M.; De Vos, D. E.; Sels, B. F.; Bossaert, W. D.; Jacobs, P. A. *Chem. Commun.* **1998**, 317.

(60) Jentys, A.; Pham, N. H.; Vinek, H. *J. Chem. Soc., Faraday Trans.* **1996**, *92*, 3287.

Table 1. BET Surface Area, Total Pore Volume, Pore Size, Loading of N, and Surface Density of N of Functionalized Mesoporous Silicas

	S_{BET} ($m^2 \cdot g^{-1}$)	V_P ($mm^3 \cdot g^{-1}$)	2 R_P[a] (nm)	N content ($mmol \cdot g^{-1}$)	N atom per nm^{-2}	fixed silane[b] per nm^{-2}
MCM-41	1283	284	2.90	0	0	0
N-MCM-41	1037	238	2.80	1.46	0.85	0.69
NN-MCM-41	586	135	2.63	2.76	2.84	0.65
NNN-MCM-41	481	111	2.52	3.53	4.42	0.55
SBA-1	1221	281	3.02	0	0	0
N-SBA-1	689	158	2.66	1.90	1.66	0.93
NN-SBA-1	606	139	2.48	3.33	3.31	0.82
NNN-SBA-1	126	36.0	2.40	4.39	21	0.72

[a] After BJH pore size distributions. [b] Based on the surface area of unfunctionalized mesoporous silicas.

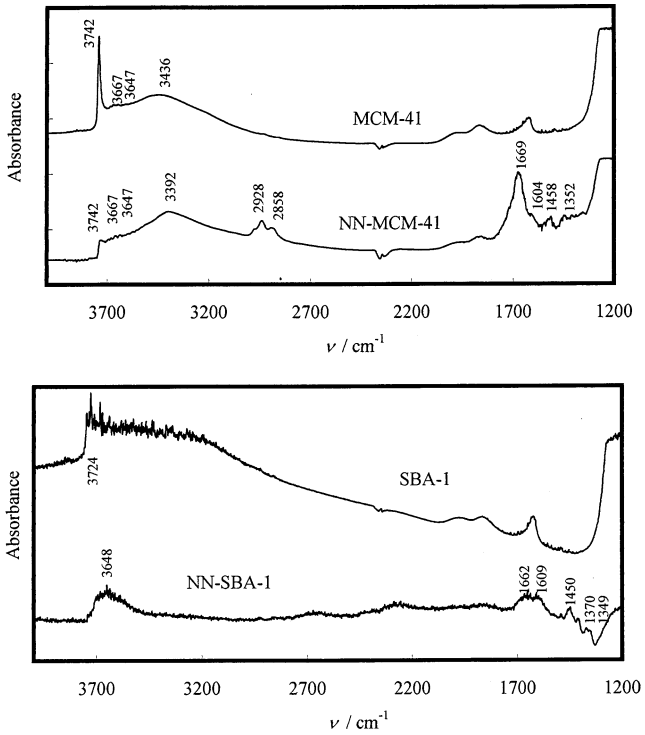

Figure 3. Infrared spectra of MCM-41 and SBA-1 overlaid with diamino-functionalized silicas.

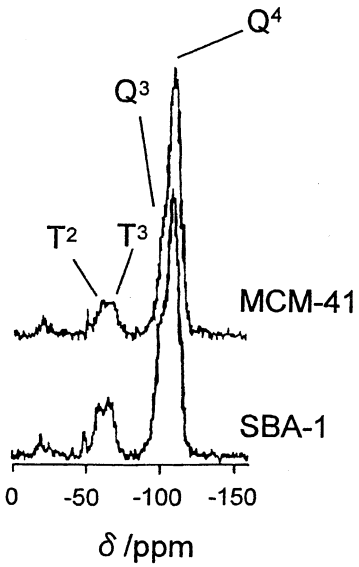

Figure 4. ^{29}Si NMR of diamino-functionalized MCM-41 and SBA-1.

Table 2. ^{29}Si Data of Functionalized Mesoporous Silicas

	relative peak area (%)						
	T^1	T^2	T^3	Q^2	Q^3	Q^4	$\Sigma T^n/\Sigma (T^n+Q^n)$
NN-MCM-41		8.2	6.2		27.8	57.7	14.4
NN-SBA-1		7.9	11.1		25.2	55.8	19.0

not observed. The integrated areas of these peaks are summarized in Table 2. The population of T^2 is larger than T^3 in NN-MCM-41, whereas T^3 is more abundant in NN-SBA-1. In contrast, the Q^3/Q^4 ratio in NN-MCM-41 and NN-SBA-1 is almost the same. The differences in the ratios of T^2/T^3 and Q^3/Q^4 demonstrate that the population of silanol generated on the attached silane is larger in MCM-41 than in SBA-1, whereas the density of silanol on the framework silicon does not differ substantially. In considering the density of Si−OH on MCM-41, one or two Si−OH can be bound to silane molecules, and $SiR(SiO)(OH)_2$ or $SiR(SiO_4)(OH)$ species form after the hydrolysis of remaining methoxy groups. If another silane attacks to react with the silane already fixed on the surface, these species turn into $SiR(SiO_4)_3$ by consuming water molecules physically adsorbed on the surface. These modes of fixation suggest that the number of T^2 species reflects that of the silane molecules directly fixed on the surface, which are as randomly distributed as the silanol groups of MCM-41. Thus, the difference in T^2/T^3 ratio between the two mesoporous substrates implies that more silanes are directly linked with each other in SBA-1, and the functional group is more randomly distributed in the pores of MCM-41 than those in SBA-1. The origin of the easier formation of Si−O−Si in SBA-1 is not explored further in this work. The ratio of silicon bound to the organic group to total silicon, $\Sigma T^n/\Sigma (T^n + Q^n)$, is larger in NN-SBA-1 than in NN-MCM-41. The ratio (19.0/14.5 = 1.3) is nearly the same as that of the number of N per unit area in the last column in Table 1 (3.31/2.84 = 1.2). All these results consistently show that the amino groups are more densely packed on SBA-1 than on MCM-41.

The reaction of the silane with silica surfaces occurs via condensation of Si−OR with surface silanols. Although the silica surface has a significant population of aggregated silanols, which are hydrogen bonded to each other, these aggregated silanols are unreactive toward silane molecules in the absence of added water.[43,56,61] The evacuation from 373 to 773 K partially removes hydrogen-bonded silanols along with the remaining free silanols.[43,56] The density of free hydroxyl groups on MCM-41 has been reported to be 0.5∼3.0 nm^{-2} [43, 56]. Assuming a random distribution of silanol on the surface, this is not high enough to fix silanes with

(61) Chen, J.; Li, Q.; Xu, R.; Xiao, F. *Angew. Chem., Int. Ed. Engl.* **1995**, *34*, 2694.

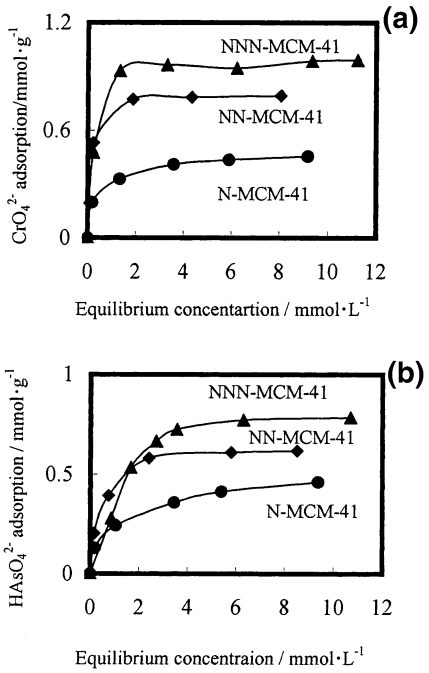

Figure 5. Adsorption isotherms of (a) arsenate and (b) chromate on functionalized MCM-41. Functionalized MCM-41 (50 mg) was stirred for 10 h in 100 mL of aqueous solutions of arsenate or chromate at room temperature.

more than two Si−O−Si bonds. (The lack of T_1 in the NMR spectra implies a lack of $Si(OH)_2$). $(T^2 + T^3)/Q^3 = 0.52$ for MCM-41 (Table 2) suggests that a significant amount of free Si−OH remains after the silylation. The average number of Si*−O−Si bonds, where Si* is the silicon from silane, is 2.1 for NN-MCM-41($2 \times 12.4\% + 3 \times 2.0\%$)/(12.4% + 2.0%) = 2.1). On the other hand, the surface density of silane on the basis of the surface area after silylation, 1.4 per nm^2 (1283 m^2·g^{-1}/586 m^2·g^{-1} × 0.65 per nm^2 = 1.4 per nm^2, data for NN-MCM-41 in Table 1), must be formed at the expense of at least 2.9 silanols per nm^2 (1.4 molecule per nm^2 × 2.1 Si−O−Si per molecule = 2.9 per nm^2). This agrees well with the surface silanol density (3.0 Si−OH per nm^2) but is totally unreasonable because a certain combination of silanols that geometrically fits to the silane molecule is necessary for the fixation to generate $Si(OH)R(OSi)_2$ and $SiR(OSi)_3$. However, on the basis of the initial surface area of the mesoporous silicas, the number of silanols used is 1.4 per nm^2. Thus, the fixation probably begins before the destruction of the mesoporous structure; the bond formation with consumption of Si−OH may be a trigger or an initiator of destruction of the framework.

Adsorptions of Chromate and Arsenate. Figure 5 shows the adsorption isotherms of chromate and arsenate on the amino-functionalized MCM-41. The slopes of the initial curves are very steep for chromate adsorptions until saturation. On the other hand, the uptake of arsenate gradually increases according to the concentration in the solution. The initial slope is not significantly dependent on the functional groups. The saturation of these oxyanions increases with increasing numbers of nitrogens on the parent silanes, which roughly corresponds to the number of amino groups in the adsorbent powder. However, the maximum adsorption is not proportional to the number of N. To explore the effect of the type of functional groups, some examples of adsorption are listed in Tables 3 and 4.

Table 3. Adsorptions of Chromate on Functionalized Mesoporous Silicas

	concentration of CrO_4^{2-}		specific ads.		
adsorbent	initial (ppm)	final (ppm)	mg/g ads.	(θ^a)	K_d^b
N-MCM-41	10.8	0.00	2.17	(0.04)	$>2.0 \times 10^5$
	30.4	0.48	5.99	(0.11)	1.24×10^4
	136.4	21.3	23.0	(0.44)	1.08×10^3
NN-MCM-41	10.8	0.00	2.17	(0.02)	$>2.0 \times 10^5$
	30.4	0.13	6.06	(0.07)	4.56×10^4
	123.3	10.0	22.7	(0.24)	2.26×10^3
NNN-MCM-41	10.8	0.00	2.17	(0.02)	$>2.0 \times 10^5$
	30.4	0.00	6.08	(0.05)	$>2.0 \times 10^5$
	304.2	27.9	55.3	(0.48)	1.98×10^3
N-SBA-1	10.8	0.78	2.01	(0.02)	2.59×10^3
	30.4	4.66	5.15	(0.05)	1.11×10^3
	151.3	46.7	20.9	(0.22)	448
NN-SBA-1	10.8	0.00	2.17	(0.01)	$>2.0 \times 10^5$
	30.4	0.06	6.07	(0.03)	9.79×10^4
	163.82	5.90	31.6	(0.17)	5.35×10^3
NNN-SBA-1	10.8	0.00	2.17	(0.01)	$>2.0 \times 10^5$
	30.4	0.00	6.08	(0.03)	$>2.0 \times 10^5$
	317.16	3.02	62.8	(0.29)	2.08×10^4

[a] Coverage = (adsorbed chromate/N)/(adsorbed chromate/N)$_{saturation}$. [b] Distribution coefficient between solid and water phase.

Table 4. Adsorptions of Arsenate on Functionalized Mesoporous Silicas

	concentration of $HAsO_4^{2-}$		specific ads.		
adsorbent	initial/ ppm	final/ ppm	mg/ g-ads.	(θ^a)	K_d^b
N-MCM-41	10.6	0.00	2.05	(0.03)	$>2.0 \times 10^5$
	30.3	2.13	5.64	(0.09)	2.64×10^3
	114.9	25.1	18.0	(0.28)	713
NN-MCM-41	10.6	0.00	2.11	(0.02)	$>2.0 \times 10^5$
	30.3	1.06	5.85	(0.07)	5.51×10^3
	164.4	21.4	28.6	(0.33)	1.34×10^3
NNN-MCM-41	10.6	0.00	2.11	(0.02)	$>2.0 \times 10^5$
	30.3	0.32	6.00	(0.05)	1.87×10^4
	316.1	30.3	57.2	(0.52)	1.89×10^3
N-SBA-1	10.6	0.16	2.08	(0.02)	1.28×10^4
	30.3	0.57	5.95	(0.04)	1.04×10^4
	204.1	28.4	35.1	(0.26)	1.23×10^3
NN-SBA-1	10.6	0.00	2.11	(0.01)	$>2.0 \times 10^5$
	30.3	0.26	6.01	(0.03)	2.29×10^4
	213.7	14.6	39.8	(0.19)	2.73×10^3
NNN-SBA-1	10.6	0.00	2.11	(0.008)	$>2.0 \times 10^5$
	30.3	0.00	6.07	(0.02)	$>2.0 \times 10^5$
	254.8	0.65	50.9	(0.19)	7.85×10^4

[a] Coverage = (adsorbed arsenate/N)/(adsorbed arsenate/N)$_{saturation}$. [b] Distribution coefficient between solid and water phase.

When the initial concentration of chromate was low enough, the oxyanion was completely removed from the solution. In this case, the distribution coefficient K_d = [anion adsorbed]/[anion in the solution] exceeded 2×10^5. Such cases were found in the data taken at an initial concentration of 10.8 ppm for N- and NN-MCM-41 and that for 10.8−30.4 ppm for NNN-MCM-41 as shown in Table 3. Because K_d strictly depends on the concentration of arsenate, the comparison among the adsorbents should be made at the same coverage. The coverage, θ, here defined as adsorbed Cr per number of N divided by its maximum, which is calculated from the data at the adsorption saturation (Table 5). The comparison of K_d at the same θ is effective in showing the actual performance of the adsorbents in the treatment

Table 5. Molar Ratio of Anion/N and Specific Adsorption at Saturation[a]

	CrO_4^{2-}		$HAsO_4^{2-}$	
	Cr/N	mg/g ads.	As/N	mg/g ads.
N-MCM-41	0.35	52.9	0.35	64.4
NN-MCM-41	0.34	92.1	0.27	86.4
NNN-MCM-41	0.32	115.2	0.25	109.9
N-SBA-1	0.47	94.2	0.55	132.7
NN-SBA-1	0.50	178.4	0.50	214.3
NNN-SBA-1	0.46	210.8	0.48	262.7

[a] Calculated from adsorption isotherms.

of water over a certain period. There are experimental difficulties in determining the initial concentration of chromate which will reach the same coverage at the adsorption equilibrium. Nevertheless, the comparison is possible between $[CrO_4^{2-}]_{initial} = 136$ ppm for N-MCM-41 and $[CrO_4^{2-}]_{initial} = 304$ ppm for NNN-MCM-41 ($\theta =$ 0.44 and 0.48, respectively) or between $[CrO_4^{2-}]_{initial} =$ 30.4 ppm for NN-MCM-41 and $[CrO_4^{2-}]_{initial} = 30.4$ ppm for NNN-MCM-41 ($\theta = 0.05$ and 0.07, respectively). In the former case, K_d for N-MCM-41 is 1.08×10^3, whereas that for NNN-MCM-41 is 2.08×10^4. The factor of enhancement was ca. 19. In the latter case, K_d for N-MCM-41 is 4.56×10^4 while that for NNN-MCM-41 is over 2.0×10^5. The factor of enhancement was more than 4.3. The difference in $K_d(\theta)$ between N- and NNN-MCM-41 can be explained by the coordination number of the ligand. On N-MCM-41, the ensemble of vicinal functional groups is necessary to neutralize the charge of CrO_4^{2-}, whereas each organic group on NNN−MCM-41 has enough amino residues to balance the charge. On the other hand, the advantage of NNN-MCM-41 to NN-MCM-41 may be attributable to the entropy gain. However, the possibility of ligating to three neighboring amino heads is three times higher than that of two neighboring heads. The deviation from the simple statistics implies a stable structure realized by NNN-ligand or a combination of proximal functional groups for capturing chromate. The same effect was also observed for the adsorbents with the SBA-1 structure.

The difference in $K_d(\theta)$ between N- and NN-mesoporous silicas is alternatively attributable to chelation of the anion.[62] In contrast, the difference between NN- and NNN-mesoporous silicas is not likely due to that of chelating effects because the enhancement of stability constant for the complex formations is not large when the ligand is changed from en to dien.

In the adsorption of arsenate, the distribution coefficient is smaller than that of chromate as shown in Table 4. However, at $[HAsO_4^{2-}]_{initial} = 10$ ppm, it reached more than 2.0×10^5 for all adsorbents. The enhancement of adsorption with increasing number of N in the parent silane is clearly demonstrated by comparing NN- and NNN-SBA-1. The enhancement of K_d was a factor of 29 at $\theta = 0.19$.

The stoichiometry of oxyanion to N and the capacity (adsorbed oxyanion in mg per adsorbent in g) are directly calculated from the amount of oxyanions at the adsorption saturation, as shown in Table 5. For functionalized SBA-1, all the stoichiometries, for both chromate and arsenate and for mono-, di-, and triamines, were nearly equal to 0.5. Considering the 1 anion−2 cations charge balance in these systems, this result implies that the interaction between the amine heads and oxyanions is ionic and all amine heads can work at the saturation. On the other hand, the stoichiometry is below 0.5 in the case of functionalized MCM-41. A decrease in stoichiometry with increasing number of N is additionally found in the arsenate adsorption. The existence of amino groups inactive to oxyanion capturing is strongly suggested for MCM-41.

The dissociation constants of chromate are $pK_{a1} = -0.7$ and $pK_{a2} = 6.52$, suggesting that the charge is duplicated at pH between 6 and 7. On the contrary, the measurement under various pHs demonstrated that the adsorption capacity of chromate on NN-MCM-41 gradually increases with the decrease of pH. At pH = 1, it reaches about twice as much as that at pH = 7. The absence of a sudden drop or rise, which is expected to appear around pH = 6.5, and the gradual change in the adsorption suggest that the solvation of chromate captured by the adsorption site is different from that in the solution. The arsenate adsorption on NN-MCM-41 showed a similar dependence on pH.

Mesostructural Influences on Adsorption. With the same silanes SBA-1 is superior to MCM-41 as a support of functional groups. To the best of our knowledge, the adsorption capacities for chromate (211 mg/g) and arsenate (263 mg/g) in SBA-1 derived adsorbents are some of the largest ever reported. The former is almost comparable to the achievement in the absorption of hexavalent chromium by condensed-tannin gel (287 mg/g dry tannin gel).[28] Fryxell et al. employed Cu^{2+} fixed in the diamino group grafting in the pore of MCM-41 as the adsorption site of chromate and arsenate.[55] In fact, *w*/*w* specific adsorption at the adsorption saturation is 120 (chromate) − 140 (arsenate) mg/g adsorbent, which is comparable to our results for diamino functionalized mesoporous silicas, 86.4−214 mg/g adsorbent. Although they claimed the unique interaction of copper with oxyanions, the amino groups in the absence of metal cations adsorb more oxyanions.

The adsorbent−adsorbate interactions are considered to be mainly ionic interactions between ammonium ion and oxyanion. In addition, hydrogen bonding plays a significant role in this attraction. The uptake of divalent anions by monoamino functionalized mesoporous silica was anticipated to be considerably lower because the surface density of amino groups is 0.85 and 1.66 nm^{-2} for N-MCM-41 and N-SBA-1, respectively, (Table 1) and the respective average distances of the silanes will be 1.1 and 0.78 nm. The length from Si to N in monoaminosilane is ca. 0.5 nm and the sizes of oxyanions are ca. 0.2 nm, suggesting about half of the amino groups cannot form coordination complexes such as NH_3^+-(oxyanion)$^{2-}-NH_3^+$ on N-MCM-41. In contrast, little difference was found between mono- and diamino functionalized MCM-41, and the oxyanion to N ratio is much larger than 0.25 for N-MCM-41. The experimental results, therefore, are not consistent with a random distribution of the functional groups in the pore, but suggest domain formations, namely, the adsorption sites congregate on parts of the surface and the other parts remain bare silica. To confirm this mesoscale structural feature in the distribution of grafted silanes, we mea-

(62) Niikura, K.; Bisson, A. P.; Anslyn, E. V. *J. Chem. Soc., Perkin Trans.* **1999**, *2*, 1111.

Table 6. Specific Adsorption[a] of Arsenate by Monoamino Functionalized MCM-41

N content ($mmol \cdot g^{-1}$)	initial concentration of $HAsO_4^{2-}$ (ppm)		
	10.5	30.3	70.0
0.56	1.8	5.3	12.0
1.31	2.1	5.6	12.3
1.58	2.1	5.7	12.6
1.74	2.1	5.8	12.8

[a] In mmol/g adsorbate.

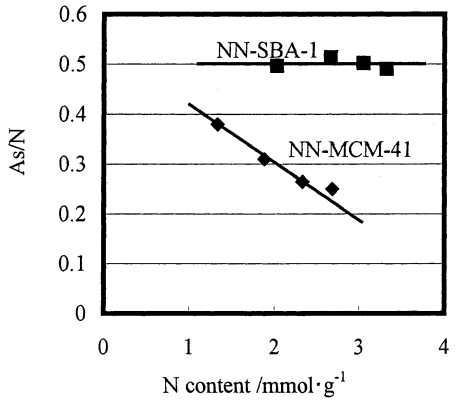

Figure 6. As/N ratio at the adsorption saturation as a function of surface density of nitrogen on NN-MCM-41 and NN-SBA-1.

sured the adsorption of arsenate on monoamino functionalized MCM-41 with various N contents. The results are shown in Table 6. At all initial $HAsO_4^{2-}$ concentrations (10.5, 30.3, and 70.0 ppm), no difference was found in resulting specific adsorptions (1.8−2.1, 5.3−5.8, and 12.0−12.8 mmol·g adsorbent^{-1}, respectively) among the mesoporous silica with various contents of N. No dependence of the specific adsorption on the surface density of amino group demonstrates the presence of functional groups in domains on the surface.

As already shown by the differences in T_2/T_3 ratios in Table 2, the silane was more randomly distributed on MCM-41, and monoamino functional groups on SBA-1 are likely to be more condensed than those on MCM-41.

The difference in the frameworks may influence the accessibility or utility of the amino groups. The As/N ratio at the adsorption saturation is plotted in Figure 6 as a function of N content. NN-SBA-1 constantly shows a stoichiometry which agrees with the charge balance of the anion to cation (As/N = 0.5). On the other hand, As/N decreases with increasing N content for NN-MCM-41, indicating that the ineffective amino groups increase with the loading amount. In a high density of functional groups, SBA-1 is a superior support to MCM-41, showing a large absorption capacity. MCM-41 and SBA-1 have considerable differences in the structure such as framework structure, chemical properties of the wall surface, etc. Because MCM-41 has pores in a straight channel which are not connected to each other, one of the likely reasons is blockage by functional groups near the pore mouths. Further studies are needed for elucidating the origin of the differences between the framework structures appearing at the saturated adsorption.

Recent developments in oxyanion absorbents have effectively utilized functionalization/modification techniques such as those with amine modified clay[34] and coconut coir.[30] In such systems, however, none of the molecular structures of the adsorption site and mesostructure are well defined. The results given for the density of adsorption sites on molecular and nano scales in our study may be a guide for designing and preparing high-performance adsorbents.

Conclusions

We have investigated the adsorption of chromate and arsenate on mono-, di-, and triamino functionalized mesoporous silicas without destroying the pore connection topologies. By the functionalization in the absence of added water, SBA-1 fixes aminosilanes more densely than MCM-41. At the low concentrations, these oxyanions are adsorbed with a distribution coefficient of more than 2.0×10^5. Triamino groups capture oxyanions more effectively than expected from the number of N, suggesting stable complex formations. At the adsorption saturation, the stoichiometries of oxyanions to N were 0.5 for all adsorbents derived from SBA-1, whereas they were 0.25−0.35 for MCM-41 derivatives. The dependence of adsorption capacity on the content of N demonstrates that SBA-1 is superior to MCM-41 because all amino groups work as adsorption sites in the former support, but not in the latter. It has been demonstrated that the functional groups are not randomly distributed but form domains on MCM-41. Knowledge of functionalized mesoporous silicas, whose structure is well analyzed, helps to build understanding of the oxyanion adsorption on molecular and meso scales.

CM0202355